Huge impact of compressive strain on phase transition temperatures in epitaxial ferroelectric K x Na 1–x NbO 3 thin films

L. von Helden, L. Bogula, P.-E. Janolin, M. Hanke, T. Breuer, M. Schmidbauer, S. Ganschow, J. Schwarzkopf

▶ **To cite this version:**

L. von Helden, L. Bogula, P.-E. Janolin, M. Hanke, T. Breuer, et al.. Huge impact of compressive strain on phase transition temperatures in epitaxial ferroelectric K x Na 1–x NbO 3 thin films. Applied Physics Letters, 2019, 114 (23), pp.232905. 10.1063/1.5094405 . hal-02169628

HAL Id: hal-02169628
https://hal.science/hal-02169628v1

Submitted on 1 Jul 2019

HAL is a multi-disciplinary open access archive for the deposit and dissemination of scientific research documents, whether they are published or not. The documents may come from teaching and research institutions in France or abroad, or from public or private research centers.

L'archive ouverte pluridisciplinaire **HAL**, est destinée au dépôt et à la diffusion de documents scientifiques de niveau recherche, publiés ou non, émanant des établissements d'enseignement et de recherche français ou étrangers, des laboratoires publics ou privés.

AIP Publishing

This manuscript was accepted by Appl. Phys. Lett. Click here to see the version of record.

Huge impact of compressive strain on phase transition temperatures in epitaxial ferroelectric $K_xNa_{1-x}NbO_3$ thin films

L. von Helden[1]*, L. Bogula[1], P.-E. Janolin[2], M. Hanke[3], T. Breuer[4], M. Schmidbauer[1], S. Ganschow[1], J. Schwarzkopf[1]

[1]*Leibniz-Institut für Kristallzüchtung, Max-Born-Str. 2, 12489 Berlin, Germany*
[2]*Laboratoire SPMS (Structures Properties and Modeling of Solids), CNRS-CentraleSupélec, Université Paris-Saclay, 8-10 rue Joliot Curie, 91190 Gif-sur-Yvette, France*
[3]*Paul-Drude-Institute for Solid State Electronics, Hausvogteiplatz 5-7, 10117 Berlin, Germany*
[4]*Fachbereich Physik, Philipps-Universität Marburg, Renthof 7, 35032 Marburg, Germany*
**corresponding author: leonard.vonhelden@ikz-berlin.de*

We present a study in which ferroelectric phase transition temperatures in epitaxial $K_xNa_{1-x}NbO_3$ films are altered systematically by choosing different (110)-oriented rare-earth scandate substrates and by variation of the potassium to sodium ratio. Our results prove the capability to continuously shift the ferroelectric-to-ferroelectric transition from monoclinic M_C to orthorhombic c-pha se by about 400 °C via application of anisotropic compressive strain. The phase transition was investigated in detail by monitoring the temperature-dependence of ferroelectric domain patterns with piezoresponse force microscopy (PFM) and upon analyzing structural changes by means of high resolution X-ray diffraction (HR-XRD) including X-ray reciprocal space mapping. Moreover, the temperature evolution of the effective piezoelectric coefficient $d_{33,f}$ was determined using double beam laser interferometry exhibiting a significant dependence on the particular ferroelectric phase.

In order to enhance functional properties in electrical applications based on ferroelectric thin films, the introduction of monoclinic unit cell symmetries via epitaxial strain was widely investigated and is by now well established.[1-9] These symmetries offer increased electromechanical properties due to enhanced polarization rotation within their monoclinic mirror planes. Besides their well-known pronounced piezoelectric response, high transmission coefficients have recently been reported for surface acoustic wave (SAW) sensors based on $K_{0.70}N_{0.30}NbO_3$ thin films grown on (110) $TbScO_3$ with selective propagation coinciding with monoclinic shearing directions.[10,11] Furthermore, a strong enhancement of SAW transmission coefficients in the vicinity of phase transition temperatures was observed. However, such transition temperatures might differ from desirable operating regimes for e.g. biosensors which calls for altering them in selective manner.

ACCEPTED MANUSCRIPT

AIP Publishing

This manuscript was accepted by Appl. Phys. Lett. Click here to see the version of record.

The key to predict and subsequently deliberately tailor phase transition temperatures in epitaxial $K_xNa_{1-x}NbO_3$ thin films is to understand the relationship between phase formation, transition temperature and incorporated lattice strain. However, no experimental investigation addressing this topic has been available for this material, yet. In this paper, we present a study in which the impact of different anisotropic epitaxial strains in $K_xNa_{1-x}NbO_3$ films on phase transition temperatures is investigated. In this context, the choice of substrate material allows for a gradual modulation of strain while the change of potassium to sodium ratio enables a continuous and precise fine tuning. Via the combination of temperature-dependent piezoresponse force microscopy (PFM), temperature-dependent in-situ X-ray diffraction (XRD) and laser interferometry we show that we can indeed continuously shift the transition from the ferroelectric, monoclinic M_C to the ferroelectric c-phase in the range of -15 °C to 400 °C.

$K_xNa_{1-x}NbO_3$ films with a thickness of 30 (±10) nm were grown on (110) $DyScO_3$, (110) $TbScO_3$, (110) $GdScO_3$ and (110) $SmScO_3$ substrates by means of liquid-delivery metal-organic vapor phase epitaxy (MOVPE). This technique allows for growth conditions close to the thermodynamic equilibrium providing smooth film surfaces and highly regular ferroelectric domain formation. The samples were prepared with a molar potassium content x ranging from 0.54 to 0.77, which was varied by adding different amounts of K and Na precursors to the MOVPE growth process, which was carried out at a growth temperature of 700 °C. Details are described in Ref. 4. The rare-earth scandate substrates have been grown by Czochralski technique as explained in Ref. 21.

(Figure 1: Lateral piezoresponse force micrographs for $K_xNa_{1-x}NbO_3$ films at room temperature presented in order of decreasing compressive strains on (a) (110) $DyScO_3$, (b) (110) $TbScO_3$, (c) (110) $GdScO_3$, (d) (110) $SmScO_3$. White double arrows indicate the orientation of stripe domains. (e) Schematic presentation of an M_C domain configuration. The in-plane polarization within the stripe domains is represented by red arrows and the resulting in-plane net polarization of superdomains by blue arrows.)

The ferroelectric domain patterns of $K_xNa_{1-x}NbO_3$ films on different substrates have been analyzed using the lateral piezoresponse force microscopy (LPFM) mode of an Asylum MFP3D-instrument with dual AC resonance tracking (DART).[12] In Figs. 1(a)-1(d) representative piezoresponse (PR=amplitude · sin(phase)) micrographs recorded at room temperature are displayed. The $K_xNa_{1-x}NbO_3$ film shown in Fig. 1(a) grown on (110) $DyScO_3$ does not exhibit a periodic domain structure at room temperature. In contrast the films presented in Figs. 1(b)-1(e) reveal periodic stripe domain patterns (indicated by white double arrows) forming up to four superdomain variants. A detailed structural analysis of the domain configuration as described in Ref. 11 proves monoclinic M_C domains with *Pm* symmetry. This structure contains four types of superdomains, which are denoted as 0°, 90°, 180° and 270° variants, as sketched in Fig. 1(e). Each of them is formed by lamellar nanodomains whose in-plane polarization components alternate by 90° as indicated by small, red arrows. The resulting in-plane net polarization of the superdomains is schematically given by blue arrows.

ACCEPTED MANUSCRIPT

AIP Publishing

This manuscript was accepted by Appl. Phys. Lett. Click here to see the version of record.

	a_{pc} (Å)	$b_{pc} = c_{pc}$ (Å)
$K_{0.50}Na_{0.50}NbO_3$[15]	3.939	3.999
$KNbO_3$[16]	3.973	4.036
	Avg. in-pl. lattice parameter (Å)	
$DyScO_3$[21]	3.949	
$TbScO_3$[21]	3.959	
$GdScO_3$[21]	3.968	
$SmScO_3$[21]	3.987	

(Table 1: Pseudocubic (pc) lattice parameters of $K_xNa_{1-x}NbO_3$ for x = 0.5 and x = 1.0 and averaged in-plane lattice parameters $(1/4 \cdot (d[1\bar{1}0]_{REScO_3}+d[001]_{REScO_3}))$ of different rare-earth scandate substrates.)

In order to determine the induced epitaxial strain in $K_xNa_{1-x}NbO_3$ thin films it is most convenient to describe the film structure in pseudocubic (pc) notation.[13] The strain state of each specimen is determined as follows: first, the variation of pseudocubic (pc) bulk lattice parameters a_{pc}, b_{pc}, and c_{pc} is calculated by applying Vegard's law[14] for 0.5 < x < 1.0 with the end members given in Table 1.[15,16] Second, we analyzed the vertical lattice parameter by X-ray diffraction, proving c_{pc}-orientation for all tested films, which allows for an evaluation of the chemical composition and thus the experienced in-plane strains ε_{xx} and ε_{yy}. Thereby, a Poisson ratio of υ = 0.38 as reported for $K_{0.5}Na_{0.5}NbO_3$ by Matsubara *et al.*[17] is applied. This calculation method was found to yield almost identical values to the alternative evaluation based on the elastic compliance. However, both methods produce a systematic uncertainty since the Poisson ratio and the elastic compliance are only available for the orthorhombic phase of $K_{0.5}Na_{0.5}NbO_3$. Nonetheless, they allow for a reliable comparison among the different $K_xNa_{1-x}NbO_3$ films investigated in this study. For the (110)-oriented rare-earth scandate ($REScO_3$) substrates the average in-plane unit cells parameters are taken (Tab. 1), since the possible in-plane unit cell orientations of the film occur with equal likelihood in an M_C domain structure. The potassium contents and in-plane strain values for the samples shown in Figs. 1(a)-1(d) are as follows: (110) $DyScO_3$ with x = 0.71, ε_{xx} = -0.1 % and ε_{yy} = -1.7 %, (110) $TbScO_3$ with x = 0.67, ε_{xx} = 0.2 % and ε_{yy} = -1.3 %, (110) $GdScO_3$ with x = 0.54, ε_{xx} = 0.6 % and ε_{yy} = -0.9 %, (110) $SmScO_3$ with x = 0.74, ε_{xx} = 0.8 % and ε_{yy} = -0.8 %.

(Figure 2: Lateral piezoresponse force micrographs for the $K_{0.66}Na_{0.34}NbO_3$ film on (110) $TbScO_3$ presented in Fig. 1(b) measured within one particular superdomain at different temperatures (a)-(d). Upon heating above 110 °C the periodic M_C domain structure vanishes until it reappears when cooling down again.)

ACCEPTED MANUSCRIPT

AIP Publishing

This manuscript was accepted by Appl. Phys. Lett. Click here to see the version of record.

In order to depict the characteristics of the phase transition in these films upon heating, its investigation by means of different techniques will be presented in the following on the example of the $K_{0.66}Na_{0.34}NbO_3$ film on (110) $TbScO_3$ which was presented in Fig. 1(b). In Figs. 2(a)-2(d) LPFM measurements recorded within one particular superdomain of the named film reveal the temperature-dependence of the ferroelectric domain pattern between 80 °C and 120 °C. Although the noise in PFM measurements increases when heating the sample, the stripe domains can be identified up to 110 °C before they abruptly vanish at 120 °C. Upon cooling back down to 110 °C the stripe domain pattern in PFM reappears, Fig. 2(d). Due to thermal drift of the sample stage it was not viable to perform temperature-dependent PFM measurements at a fixed sample position, e.g., at a superdomain boundary recording different superdomains at once. However, individual investigations of the particular superdomains proved that all variants vanish at the same temperature as expected for an M_C domain structure where all superdomains hold the same overall in-plane strain, which we define as $(\varepsilon_{xx} + \varepsilon_{yy})$.

(Figure 3: (a) Vertical lattice parameter of the $K_{0.66}Na_{0.34}NbO_3$ film shown in Fig. 1(b) and Fig. 2 and of the $TbScO_3$ substrate versus temperature. (b)-(c) X-ray reciprocal space maps in the vicinity of the $(44\bar{4})_{TSO}$ Bragg reflection at 25 °C and 150 °C, respectively.)

For a more detailed determination of the observed phase transition we have conducted temperature-dependent X-ray diffraction experiments. High-resolution X-ray diffraction (HRXRD) under elevated temperatures was performed on a diffractometer equipped with an 18-kW rotating-anode generator in Bragg-Brentano geometry and using synchrotron radiation at the PHARAO beamline of BESSY II. Additional measurements under cryogenic temperatures were performed on a Bruker Discover D8 diffractometer equipped with a Bruker MTC-Lowtemp stage. Furthermore, X-ray reciprocal space mappings (RSMs) were collected at the KMC2 beamline of BESSY II applying an Anton Paar DHS 1100 hot stage.

As known from several studies on various ferroelectric oxide materials like $K_xNa_{1-x}NbO_3$, $BaTiO_3$ or $PbTiO_3$ the thermal expansion coefficients in different crystalline phases of ferroelectrics significantly differ, which allows identifying phase transitions.[18,19,20] In Fig. 3(a) the evolution of the vertical lattice parameter of the $K_{0.66}Na_{0.34}NbO_3$ film presented in Fig. 1(a) and Fig. 2, and of the underlying (110) $TbScO_3$ substrate are shown in dependence of the temperature. While the substrate reveals a rather linear thermal expansion with an expansion coefficient of about 7×10^{-6} K^{-1} well compatible with literature values,[21] a distinct change of the slope is observed which corresponds to the phase transition in the $K_{0.66}Na_{0.34}NbO_3$ film. The position of the kink at 115 °C is in good agreement with the phase transition temperature observed by means of LPFM. Below 115 °C the vertical lattice parameter strongly increases. For T > 115 °C the curve is clearly flattened which indicates a very small or even negative thermal expansion. This effect is known for ferroelectrics like $PbTiO_3$[22] or $BaTiO_3$[23] and is attributed to the spontaneous volume ferroelectrostriction.[22,24,25] While this effect is present in both phases, its impact is more pronounced when the polarization vector coincides with the measured unit cell axis. As here the vertical lattice parameter is measured, this indicates a transition into a c-phase where the polarization vector is aligned along the c-axis of the unit cell.

ACCEPTED MANUSCRIPT

AIP Publishing

This manuscript was accepted by Appl. Phys. Lett. Click here to see the version of record.

In order to clarify the film structure below and above the phase transition, temperature-dependent X-ray reciprocal space mappings were performed in the vicinity of the asymmetric $(44\bar{4})_{TSO}$ substrate Bragg reflection containing both in-plane and out-of-plane scattering vector components, as shown in Figs. 3(b) and 3(c). At room temperature, the intensity distribution consists of a complex diffraction pattern resulting from the periodic arrangement of the M_C domains. Their monoclinic shearing can be identified from the different vertical positions of the two satellite branches (dashed, white lines), which do not intersect in their center position (red dot).[11] At 150 °C well above the transition temperature, this diffraction pattern has vanished confirming the absence of a periodic domain structure in agreement with the LPFM images shown in Fig. 2. Meanwhile, the center position of the X-ray intensity scattered by the film is still at the same in-plane $q_{00\bar{1}}$ position as the $(44\bar{4})_{TSO}$ substrate Bragg reflection proving that the film does not undergo any plastic relaxation but perfectly preserves its fully strained relation to the substrate. However, no peak splitting can be identified in the intensity pattern anymore. This implies the absence of a monoclinic distortion, proving an orthorhombic symmetry of the $K_xNa_{1-x}NaNbO_3$ unit cells in the high temperature phase. Note that the (110) $TbScO_3$ surface exhibits an anisotropic unit cell, so no tetragonal symmetry is possible in the clamped layer.

(Figure 4: Macroscopic effective vertical piezoelectric coefficient $d_{33,f}$ as function of temperature measured for a $K_{0.58}Na_{0.42}NbO_3$ film on a $SrRuO_3$ bottom electrode layer grown on (110) $TbScO_3$.)

To evaluate the ferroelectric properties below and above the phase transition, macroscopic measurements of the effective, vertical piezoelectric coefficient $d_{33,f}$ were performed with an aixACCT double beam laser interferometer in combination with a TF Analyzer 2000 and a Linkam HFS temperature stage. Thereby, so-called small-signal measurements were conducted by superimposing an AC electric field with 0.2 V amplitude and a frequency of 1 kHz to a DC field, which was gradually varied in the range of ±0.5 V.[26] This technique allows one to identify the material's response mainly caused by the intrinsic reverse piezoelectric effect. The measurements were conducted for a $K_{0.58}Na_{0.42}NbO_3$ film on a previously grown $SrRuO_3$ bottom electrode layer on (110) $TbScO_3$ with Pt top electrodes.

In Fig. 4, the evolution of the piezoelectric coefficient $d_{33,f}$ is displayed in the temperature range between 20 °C and 180 °C. From room temperature up to 50 °C $d_{33,f}$ is fairly constant with a value of 18 (±1) pm/V, which is comparable to values for clamped, lead-free $BaTiO_3$ thin films.[27] Above this temperature until 70 °C a distinct decrease is observed. For the high temperature c-phase an effective piezoelectric coefficient of 7 (±2) pm/V is found. This behavior is in good agreement with the expectation to gain the highest piezoelectric response for the monoclinic phase. We further note that the low transition temperature in this particular sample might be attributed to screening charges in the additional metallic intermediate layer, which are known to stabilize tetragonal phases.[28-30] Accordingly, PFM measurements confirm the transition from a periodic stripe pattern to an irregular domain arrangement below 60 °C (insets in Fig. 4).

ACCEPTED MANUSCRIPT

AIP Publishing

This manuscript was accepted by Appl. Phys. Lett. Click here to see the version of record.

(Figure 5: Phase transition temperature of the M_C to c-phase transition versus overall in-plane strain for $K_xNa_{1-x}NbO_3$ films with x varying between 0.54 and 0.77 grown on different (110)-oriented rare-earth scandate substrates. Blue, red, violet and green color indicate the use of $DyScO_3$, $TbScO_3$, $GdScO_3$, and $SmScO_3$ substrates, respectively. The transition temperatures have been determined by LPFM (circles), via the kink in thermal expansion measurements (stars) and by X-ray RSMs (squares).)

Summarizing the PFM, HR-XRD and interferometer results, we conclude a thermally induced phase transition from the ferroelectric, monoclinic M_C phase into a ferroelectric, orthorhombic c-phase in $K_xNa_{1-x}NbO_3$ films on (110) $TbScO_3$. From several experimental and theoretical studies, it is well-known that the phase transition temperature in a ferroelectric material can be systematically shifted by the application of strain.[31-33] Therefore, we have grown several $K_xNa_{1-x}NbO_3$ thin films with a molar potassium content x ranging from 0.54 and 0.77 on different rare-earth scandate substrates (without intermediate bottom electrode). In Fig. 5 the phase transition temperatures for $K_xNa_{1-x}NbO_3$ films with an overall compressive in-plane strain between -1.8 % and 0.0 % recorded by means of different techniques are gathered. We remark that all provided strain values were calculated for room temperature. The strain change upon temperature variation due to stronger thermal expansion coefficients of the substrates compared to the layers is less than 0.1 % per 100 K. The evolution of the transition temperature with increasing compressive strain unveils a systematic and apparently linear dependence, whereby a shift over a wide temperature range from -15 °C to 400 °C was experimentally realized. The lowest phase transition temperature is found for the $K_{0.71}Na_{0.29}NbO_3$ film on (110) $DyScO_3$ being significantly below room temperature. In contrast, the highest phase transition temperature, which is observed for the $K_{0.74}Na_{0.26}NbO_3$ film on $SmScO_3$, is already in the vicinity of the Curie temperature of bulk $K_{0.5}Na_{0.5}NbO_3$ of T_C = 415 °C.[34] However, we suppose to observe a ferroelectric-to-ferroelectric phase transition also in this case. Even though this sample is assigned a zero overall in-plane strain, it is fully epitaxially and highly anisotropically strained with ε_{xx} = 0.8 % and ε_{yy} = -0.8 %. It is widely accepted that any strain, which draws the unit cell symmetry away from being cubic, leads to an increase of the Curie temperature in perovskite-like ferroelectrics. For this reason, the ferroelectric-to-paraelectric phase transition in the layer is expected to have a significantly higher T_C than the unstrained bulk material. In between the $DyScO_3$ and $SmScO_3$ samples the influence of the varying molar potassium amount can be nicely obtained by comparing the different $K_xNa_{1-x}NbO_3$ films on, e.g., (110) $GdScO_3$. Here, the variation of x between 0.54 and 0.77, which corresponds to a change of the overall in-plane strain from -1.0 % to -0.3 %, leads to a shift of the phase transition temperature from 105 °C to 300 °C. We further note that the slope of the phase transition temperature versus overall in-plane strain (ca. 200 °C/%) is in quite good agreement with calculations recently published by Zhou *et al.*.[35] However, we underline the restricted comparability between both studies, since Zhou *et al.* conducted their theoretical investigation on isotropically strained monodomain $K_{0.5}Na_{0.5}NbO_3$ revealing an M_A to c-phase transition. In contrast, the system of anisotropically strained $K_xNa_{1-x}NbO_3$ films with polydomain configuration as present in our films holds a distinctly higher complexity.

In summary, we have studied a thermally induced phase transition in $K_xNa_{1-x}NbO_3$ thin films with $0.54 < x < 0.77$ grown by MOVPE. Compressive strains were varied between -1.8 % and 0.0 % by using different (110)-oriented $RESCO_3$ substrates (with Re = Dy, Tb, Gd, Sm). By applying

ACCEPTED MANUSCRIPT

AIP Publishing

This manuscript was accepted by Appl. Phys. Lett. Click here to see the version of record.

temperature-dependent PFM, different X-ray diffraction methods and laser interferometry we verified a ferroelectric-to-ferroelectric phase transition from monoclinic to orthorhombic symmetry in these films. Thereby, a linear correlation between the phase transition temperature and the applied overall in-plane lattice strain has been revealed. Our results underline the great potential to strain engineer $K_xNa_{1-x}NbO_3$ layers for technological application. The detailed knowledge of the relation between lattice strain, phase formation and phase transition temperature will enable the customization of functional properties like the transmission coefficients to the particular temperature regime in which an SAW sensor is desired to operate.

We thank DFG (project funding reference FE 1438|2-1) and EFRE (Project number 1.8/15) for funding the project. We further thank A. Kwasniewski, D. Többens, Z. Cheng, and T. Demuth for assistance with X-ray measurements and M. Klann for MOCVD sample preparation. We are grateful to BESSY (KMC-2 projects 17206091-ST, 18106401-ST, and in-house research at PHARAO) for providing beam time. Finally, we acknowledge J. Boschker and R. Wördenweber for fruitful discussion.

References

[1] P.-E. Janolin, J. Mater. Sci. **44**, 5025 (2009).

[2] D. Vanderbilt and M. H. Cohen, Phys. Rev. B **63**, 094108 (2001).

[3] G. Bai and W. Ma, Physica B **405**, 1901 (2010).

[4] J. Schwarzkopf, D. Braun, M. Hanke, R. Uecker, and M. Schmidbauer, Front. Mater. **4**, 26 (2017).

[5] V.G. Koukhar, N.A. Pertsev, and R. Waser, Phys. Rev. B **64**, 214103 (2001).

[6] Z. Chen, Z. Luo, C. Huang, Y. Qi, P.Yang, L. You, C. Hu, T. Wu, J. Wang, C. Gao, T. Sritharan, and L. Cheng, Adv. Funct. Mater. **21**, 133 (2011).

[7] J. Schwarzkopf, D. Braun, M. Hanke, A. Kwasniewski, J. Sellmann, and M. Schmidbauer, J. Appl. Cryst. **49**, 375 (2016).

[8] M. Schmidbauer, D. Braun, T. Markurt, M. Hanke, and J. Schwarzkopf, Nanotechnology **28**, 24LT02, (2017).

[9] D. Braun, M. Schmidbauer, M. Hanke, and J. Schwarzkopf, Nanotechnology **29**, 015701 (2018).

[10] S. Liang, Y. Dai, L. von Helden, J. Schwarzkopf, and R. Wördenweber, Appl. Phys. Lett. **113**, 052901, (2018).

[11] L. von Helden, M. Schmidbauer, S. Liang, M. Hanke, R. Wördenweber, and J. Schwarzkopf, Nanotechnology **29**, 415704, (2018).

[12] A. Gannepalli, D. G. Yablon, A. H. Tsou, R. Proksch, Nanotechnology **22**, 355705 (2011).

[13] A. Vailionis, H. Boschker, W. Siemons, E. P. Houwman, D. A. Blank, G. Rijnders, and G. Koster, Phys. Rev. B **83**, 064101 (2011).

ACCEPTED MANUSCRIPT

AIP Publishing

This manuscript was accepted by Appl. Phys. Lett. Click here to see the version of record.

[14] A. R. Denton, and N. W. Ashcroft, Phys. Rev. A 43, 3161 (1991).

[15] L. Wu, J. L. Zhang, C. L. Wang, and J. C. Li, J. Appl. Phys. **103**, 084116 (2008).

[16] A. G. Kalinichev, J.D. Bass, C. S. Zha, P. D. Han, and D. A. Payne, J. Appl. Phys. **74**, 6603 (1993).

[17] M. Matsubara, T. Yamaguchi, K. Kikuta, and S. Hirano, Jpn. J. Appl. Phys. **44**, 6136-6142 (2005).

[18] B. Malic, H. Razpotnik, J. Koruza, S. Kokalj, J. Cilenšek, and M. Kosec, J. Am Ceram. Soc. **94**, 2273-2275 (2011).

[19] K. Shibata, K. Suenaga, A. Nomoto, and T. Mishima, Jap. J. Appl. Phys. **48**, 121408 (2009).

[20] I. C. Infante, S. Lisenkov, B. Dupé, M. Bibes, S. Fusil, E. Jacquet, G. Geneste, S. Petit, A. Courial, J. Juraszek, L. Bellaiche, A. Barthélémy, and B. Dkhil, Phys. Rev. Lett. **105**, 057601 (2010).

[21] R. Uecker, B. Velickov, D. Klimm, R. Bertram, M. Bernhagen, M. Rabe, M. Albrecht, R. Fornari, and D. G. Schlom, J. Cryst. Growth **310,** 2649 (2008).

[22] J. Chen, K. Nittala, J. S. Forrester, J. L. Jones, J. Deng, R. Yu, and X. Xing, J. Am. Chem. Soc. **133**, 11114 (2011).

[23] G. Shirane, and A. Takeda, J. Phys. Soc. Jpn. **7**, 1 (1952).

[24] J. Chen, L. Hu, J. Deng, and X. Xing, Chem. Soc. Rev. **44**, 3522 (2015).

[25] Z. Pan, J. Chen, X. Jiang, L. Hu, R. Yu, H. Yamamoto, T. Ogata, Y. Hattori, F. Guo, X Fan, Y. Li, G. Li, H. Gu, Y. Ren, Z. Lin, M. Azuma, and X. Xing, J. Am. Chem. Soc. **139**, 14865 (2017).

[26] D. Bolten, U. Böttger, and R. Waser, J. Appl. Phys. **93**, 1735 (2003).

[27] B. Negulescu, C.J.M. Daumont, J. Sakai, A. Ruyter, M. Bavencoffe, N. Alyabyeva, and J. Wolfman, Ferroelectrics **514**, 9-18 (2017).

[28] D. Sichuga, I. Ponomareva, and L. Bellaiche, Phys. Rev. B **80**, 134116 (2009).

[29] N. A. Pertsev, and H. Kohlstedt, Phys. Rev. Lett. **98**, 257603 (2007).

[30] B. Darinskii, A. Sidorkin, A. Sigov, and N. Popravko, Materials **11**, 85 (2018).

[31] K. J. Choi, M. Biegalski, Y. L. Li, A. Sharan, J. Schubert, R. Uecker, P. Reiche, Y.B. Chen, X. Q. Pan, V. Gopalan, L.Q. Chen, D. G. Schlom, and C. B. Eom, Science **306**, 1005 (2004).

[32] J. H. Haeni, P. Irvin, W. Chang, r. Uecker, P. Reiche, Y. L. Li, S. Choudhury, W. tian, M. E. Hawley, B. Craigo, A. K. Tagantsev, X. Q. Pan, S. K. Streiffer, L. Q. chen, S. W. Kirchoefer, J. Levy, and D. G. Schlom, Nature **430**, 758 (2004).

[33] N. A. Pertsev, A. K. Tagantsev, and N. Setter, Phys. Rev. B **61**, R825 (2000).

[34] J.-F. Li, K. Wang, F.-Y. Zhu, L.-Q. Cheng, and F.-Z. Yao, J. Am. Ceram. Soc. 96, 3677-3696 (2013).

[35] M.-J. Zhou, J.-J. Wang, L.-Q. Chen, and C.-W. Nan, J. Appl. Phys. **123**, 154106 (2018).

ACCEPTED MANUSCRIPT

AIP Publishing

This manuscript was accepted by Appl. Phys. Lett. Click here to see the version of record.

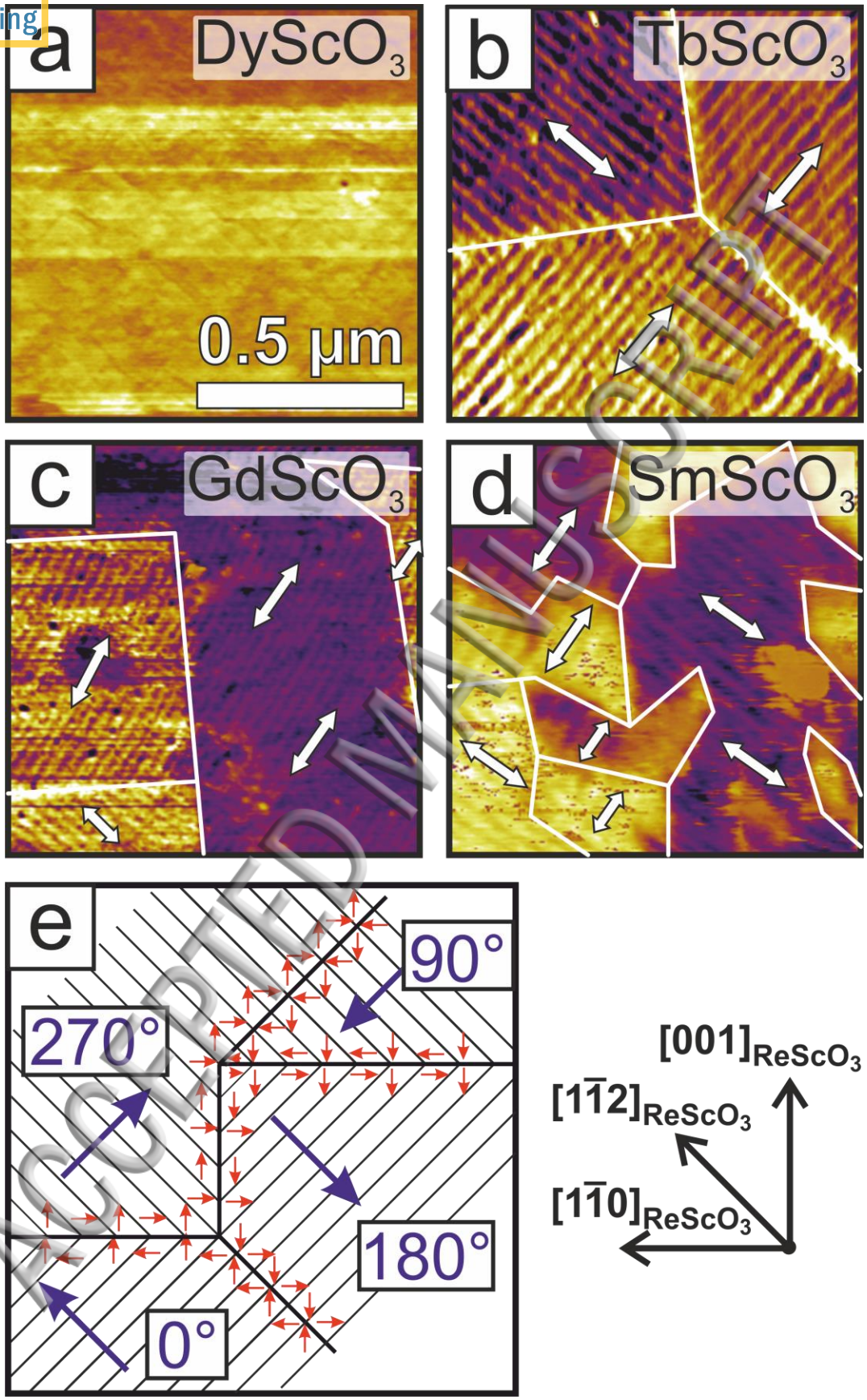

ACCEPTED MANUSCRIPT

AIP Publishing

This manuscript was accepted by Appl. Phys. Lett. Click here to see the version of record.

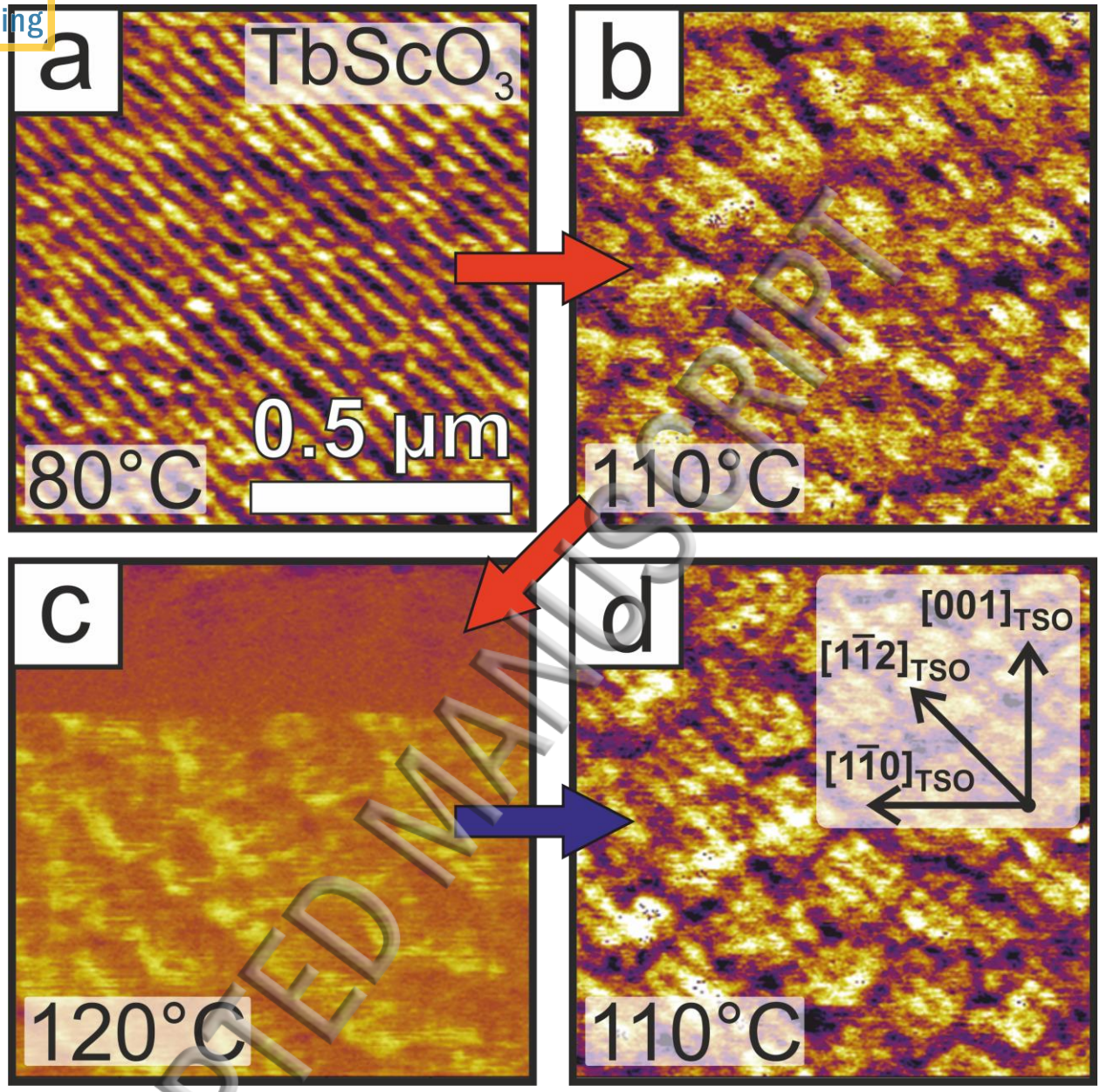

ACCEPTED MANUSCRIPT

AIP Publishing

This manuscript was accepted by Appl. Phys. Lett. Click here to see the version of record.

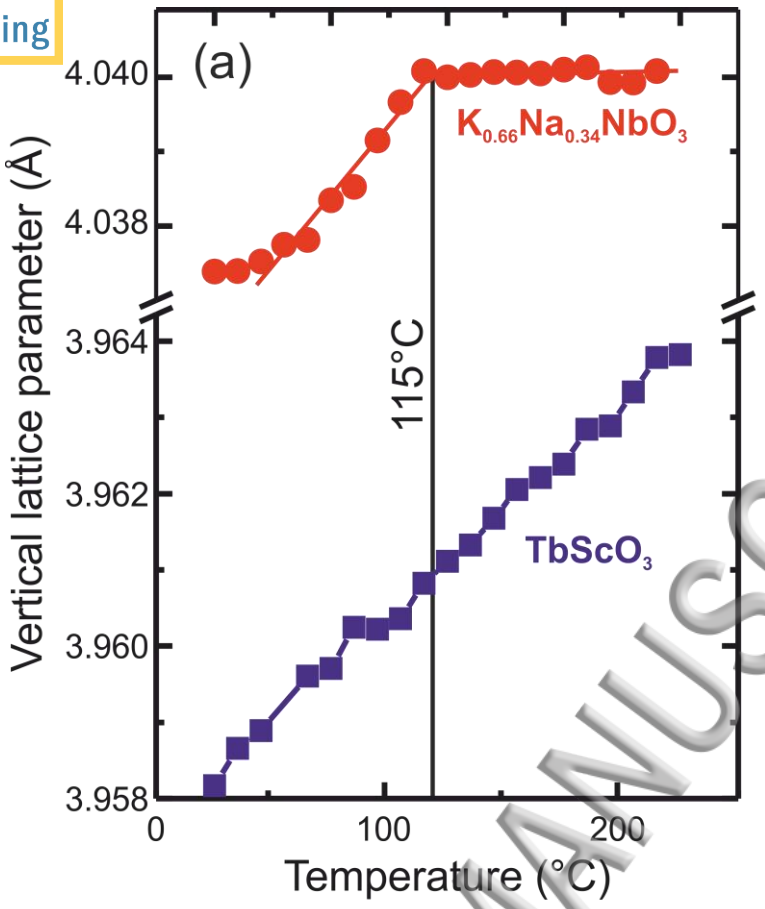

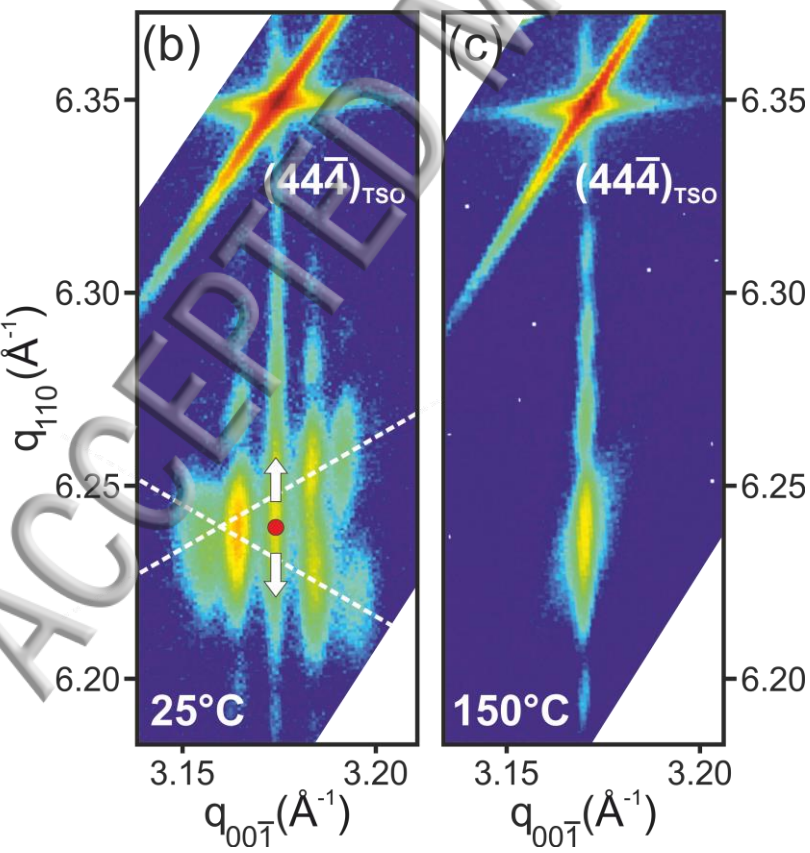

ACCEPTED MANUSCRIPT

AIP Publishing

This manuscript was accepted by Appl. Phys. Lett. Click here to see the version of record.

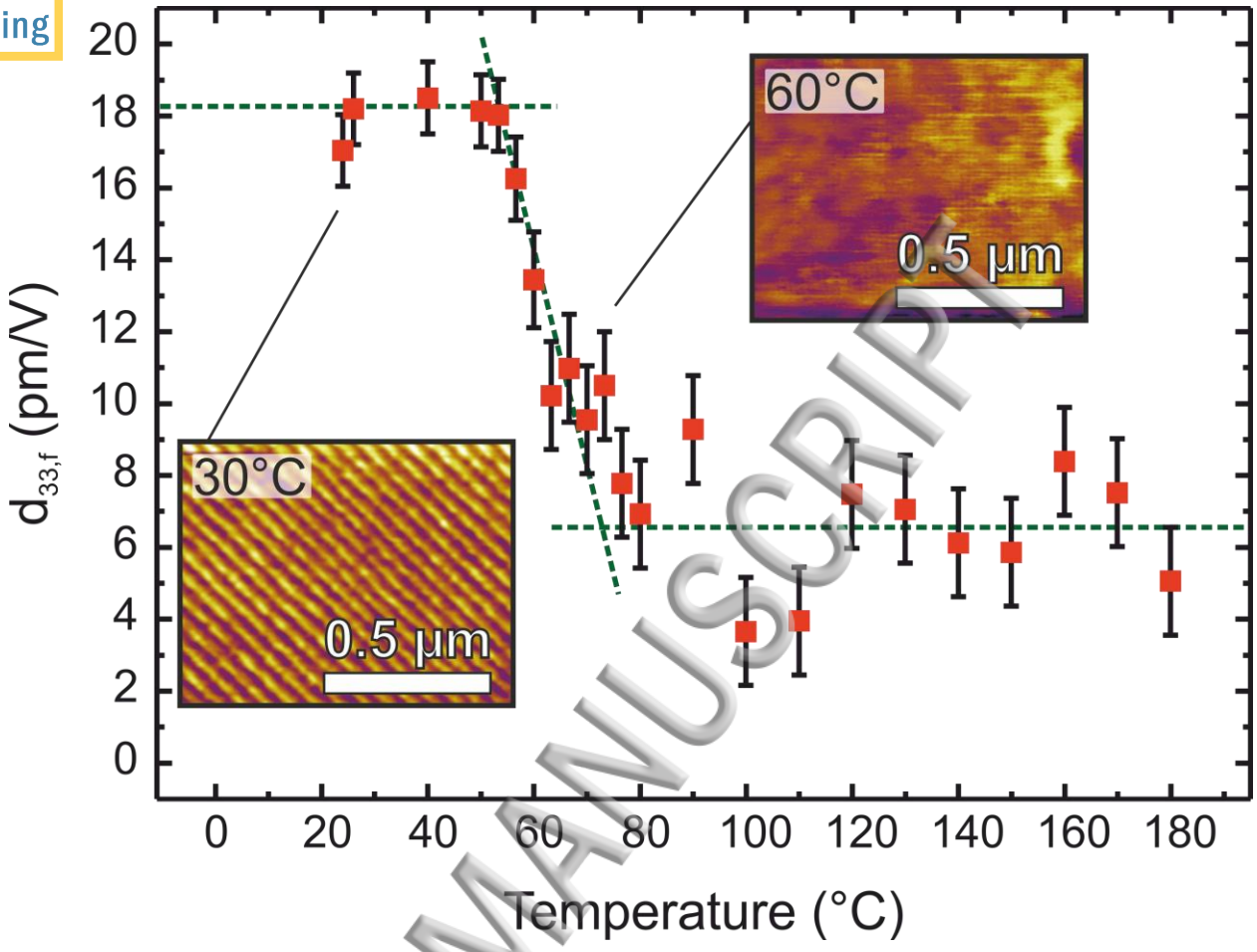

ACCEPTED MANUSCRIPT

AIP Publishing

This manuscript was accepted by Appl. Phys. Lett. Click here to see the version of record.

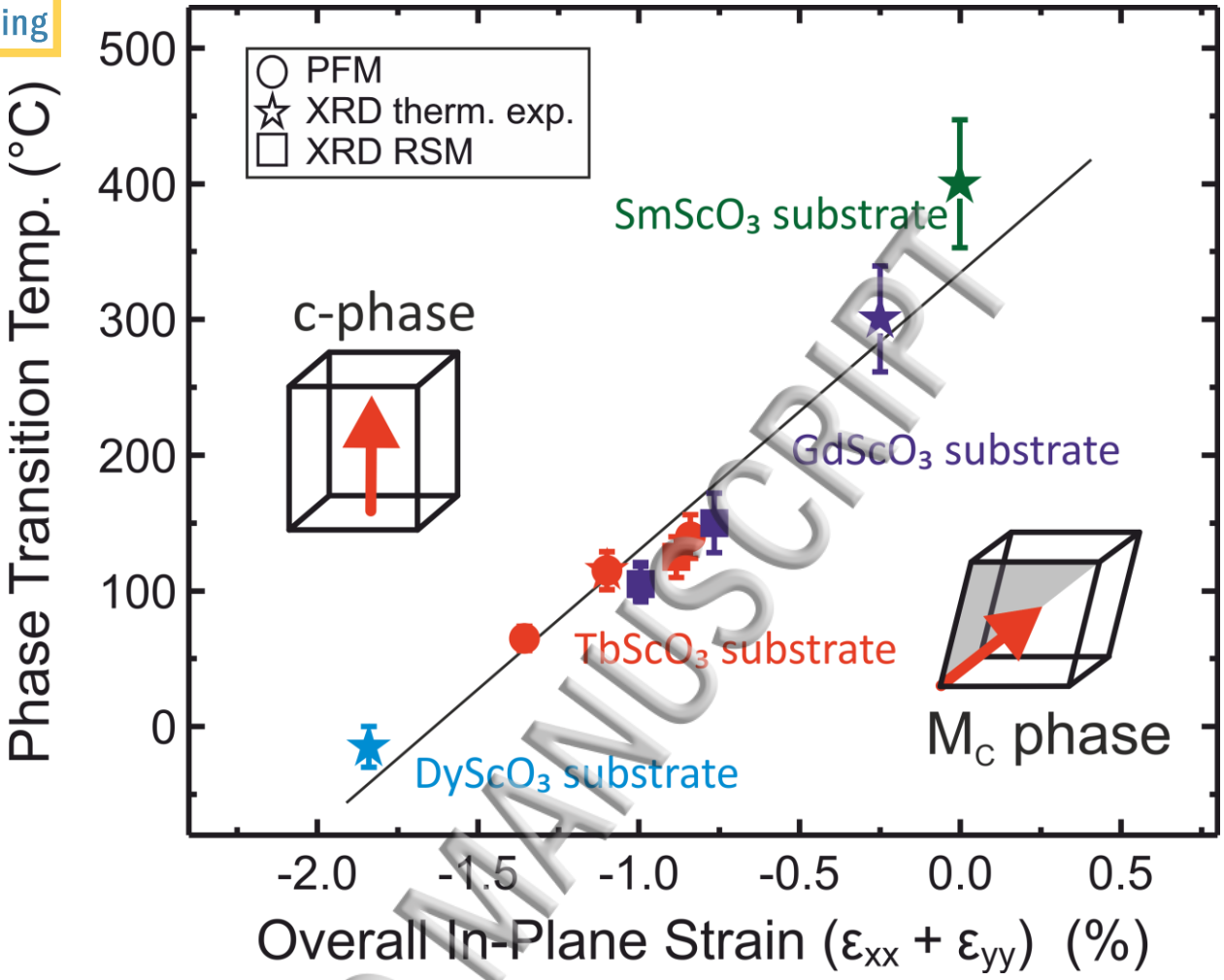

ACCEPTED MANUSCRIPT